Hibbs, M. S., Hoidal, J. R., & Kang, A. H. (1987) *J. Clin. Invest. 80*, 1644–1650.
Laemmli, U. K. (1970) *Nature 227*, 680–685.
Liotta, L. A., Rao, C. N., & Barsky, S. H. (1983) *Lab. Invest. 49*, 636–649.
Lyons, J. G., Nethery, A., O'Grady, R. L., & Harrop, P. J. (1989a) *Matrix 9*, 7–16.
Lyons, J. G., Siew, K., & O'Grady, R. L. (1989b) *Int. J. Cancer 43*, 119–125.
McKinney, M. M., & Parkinson, A. (1987) *J. Immunol. Methods 96*, 271–278.
Merril, C. R., Goldman, D., Sedman, S. A., & Ebert, M. H. (1980) *Science 211*, 1437–1438.
Muller, D., Quantin, B., Gesnel, M.-C., Millom-Collard, R., Abecassis, J., & Breathnach, R. (1988) *Biochem. J. 253*, 187–192.
Murphy, G., Bretz, U., Baggiolini, M., & Reynolds, J. J. (1980) *Biochem. J. 192*, 517–525.
Murphy, G., Ward, R., Hembry, R. Reynolds, J. J., Kuhn, K., & Tryggvason, K. (1989) *Biochem. J. 258*, 463–472.
O'Grady, R. L., Upfold, L. I., & Stephens, R. W. (1981) *Int. J. Cancer 28*, 509–515.
O'Grady, R. L., Nethery, A., & Hunter, N. (1984) *Anal. Biochem. 140*, 490–494.
Okada, Y., Nagase, H., & Harris, E. D., Jr. (1986) *J. Biol. Chem. 261*, 14245–14255.
Sanchez-Lopez, R., Nicholson, R., Gesnel, M.-C., Matrisian, L. M., & Breathnach, R. (1988) *J. Biol. Chem. 263*, 11892–11899.
Sopata, I., & Dansewicz, A. M. (1974) *Biochim. Biophys. Acta 370*, 510–523.
Springman, E. B., Angleton, E. L., Birkedal-Hansen, H., & Van Wart, H. E. (1990) *Proc. Natl. Acad. Sci. U.S.A. 87*, 364–368.
Stevenson, G. A., Lyons, J. G., Cameron, D. A., & O'Grady, R. L. (1985) *Biosci. Rep. 5*, 1071–1077.
Tyler, J. M., & Branton, D. (1980) *J. Ultrastruct. Res. 71*, 95–102.
Vartio, T., Hovi, T., & Vaheri, A. (1982) *J. Biol. Chem. 257*, 8862–8866.
Vissers, M. C. M., & Winterbourn, C. C. (1988) *Collagen Relat. Res. 8*, 113–122.
Whitham, S. E., Murphy, G., Angel, P., Rahmsdorf, H.-J., Smith, B. J., Lyons, A., Harris, T. J. R., Reynolds, J. J., Herrlich, P., & Docherty, A. J. P. (1986) *Biochem. J. 240*, 913–916.
Wilhelm, S. M., Collier, I. E., Marmer, B. L., Eisen, A. Z., Grant, G. A., & Goldberg, G. I. (1989) *J. Biol. Chem. 264*, 17213–17221.
Windsor, L. J., Birkedal-Hansen, H., Birkedal-Hansen, B., & Engler, J. (1990) in *Matrix, Collagen and Related Research, Special Issue* (Birkedal-Hansen, H., Werb, Z., Welgus, H. G., & Van Wart, H., Eds.) Gustav Fischer Verlag, Stuttgart, Germany (in press).
Yamagata, S., Ito, Y., Tanaka, R., & Shimizu, S. (1988) *Biochem. Biophys. Res. Commun. 151*, 158–162.
Yamamoto, K., Sekine, T., & Kanaoka, Y. (1977) *Anal. Biochem. 79*, 83–94.

Kinetic Evidence for Two Nucleotide Binding Sites on the CaATPase of Sarcoplasmic Reticulum†

Richard J. Coll* and Alexander J. Murphy
Department of Biochemistry, School of Dentistry, University of the Pacific, San Francisco, California 94115
Received July 30, 1990; Revised Manuscript Received October 1, 1990

ABSTRACT: The CaATPase of sarcoplasmic reticulum was reacted with [γ-^{32}P]ATP to form the covalent phosphoenzyme intermediate. Noncompetitive inhibition by reactive red-120 and chelation of calcium allowed us to monitor single-turnover kinetics of the phosphoenzyme reacting with water or added ADP at 0 °C. When ADP was added and the amount of product, [γ-^{32}P]ATP, formed was measured, we found that added cold ATP did not interfere with the phosphoenzyme reacting with ADP. We conclude that ATP cannot bind where ADP binds, the phosphorylated active site. This implies that when ATP at high concentrations causes an acceleration of phosphoenzyme hydrolysis, it must do so by binding to an allosteric site. Considering the monoexponential nature of product formation we observed, simple one-nucleotide-site models cannot account for the above result.

The ATPase of sarcoplasmic reticulum (SR)[1] membranes is an ionmotive pump which functions in myocytes to transport calcium from the cytosol to the membrane lumen (de Meis, 1981; Inesi 1985; Kirtley et al., 1990). In common with other membrane ATPases, it shows complex dependence of the velocity of ATP hydrolysis on substrate concentration (Inesi et al., 1967; Yamamoto & Tonomura, 1967), so that nonlinear Lineweaver–Burk and Eadie–Hofstee plots are obtained (non-Michaelis–Menten behavior). Among related enzymes with this property are the proton pumps of mitochondria (Schuster et al., 1975) and chloroplasts (Bowman, 1983; Koland & Hammes, 1986), the plasma membrane cation ATPases of the sodium–potassium (Kanazawa et al., 1978;

† This research was supported by Grant GM 31083 from the National Institutes of Health.

[1] Abbreviations: SR, sarcoplasmic reticulum; Ap_5A, P^1,P^5-bis(5′-adenosyl) pentaphosphate; Mops, 3-(*N*-morpholino)propanesulfonic acid; EGTA, ethylene glycol bis(β-aminoethyl ether)-*N*,*N*,*N*′,*N*′-tetraacetic acid; EP, phosphorylated enzyme intermediate; FITC, fluorescein isothiocyanate (isomer I).

0006-2960/91/0430-1456$02.50/0

Post et al., 1972), proton–potassium (Wallmark et al., 1980), and calcium (Richards et al., 1978; Stieger & Luterbacher, 1981) types, and the MgATPase of transverse tubules (Moulton et al., 1986). Although the biological significance of this complex behavior is not presently known, clarifying its origin would provide valuable structural and mechanistic insights.

A number of hypotheses have been proposed to account for the complex behavior of these ATPases. These include (a) alternating-site cooperativity (Hutton & Boyer, 1979; Gresser et al., 1982), (b) a single active site existing in high- and low-affinity forms (Moczydlowski & Fortes, 1981), (c) a single site which, after it is phosphorylated, can bind ATP with low affinity so that subsequent steps are accelerated (Champeil et al., 1988; Bishop et al., 1987), and (d) the presence of a second distinct nucleotide site (Coll & Murphy, 1985). In this report, we describe experiments which show that cold ATP accelerates rather than inhibits the synthesis of [γ-^{32}P]ATP from the phosphorylated enzyme and ADP. Since this cold ATP and ADP cannot occupy the same site, these results support the existence of an allosteric site distinct from the active site.

Materials and Methods

SR vesicles were prepared from rabbit hind leg white muscle according to the method of Eletr and Inesi (1972). [^{32}P]P_i and [γ-^{32}P]ATP were from ICN. ATP, ADP, reactive red-120, phosphoenolpyruvate, pyruvate kinase, and Ap_5A were all from Sigma. All other chemicals were reagent grade or better.

Measurements of the Levels of EP and the Rate of Their Decomposition. All reactions were carried out at 0 °C. To a solution of 0.28 mg/mL SR, 2.8 μM reactive red-120 (10 nmol/mg of SR protein), 8 μM Ap_5A, 80 mM KCl, 50 mM Mops, pH 7.0, 5 mM $MgCl_2$, 1.1 mM $CaCl_2$, and 1.0 mM EGTA was added 25 μM (final) [γ-^{32}P]ATP. A zero time point was obtained by removing a 900-μL aliquot of the reaction solution and adding it to 200 μL of ice-cold 25% TCA in a 1.5-mL microcentrifuge tube. To initiate the EP decomposition reaction, 6 mM (final) EGTA was added, and at given times, 900-μL aliquots were quenched as described above. The samples were centrifuged at 2000 rpm for 5 min, and the drained pellets were subsequently washed twice with 1 mL of ice-cold 5% TCA/1 mM P_i. The pellets in the microcentrifuge tubes were placed in scintillation vials, 2.5 mL of Ecolume (ICN) was added, and they were counted directly.

When the effect of added nucleotides on EP decomposition was studied, they were added as their Mg complexes along with EGTA at time zero. When the effect of ATP on EP decomposition was studied, the reaction mixtures also contained 2 mM phosphoenolpyruvate and 5 IU of pyruvate kinase in addition to the previously mentioned components. This latter precaution is necessary since the uninhibited calcium-independent ATPase present in SR might produce significant hydrolysis of ATP during these time courses.

Measurements of P_i Production and ATP Synthesis. To measure the products of EP decomposition, we used the observation of Dupont (1984) that the SR membranes embedded in Millipore (HAWP, 0.45 μm) filters behave the same as in solution. We used a handmade vacuum filtration apparatus to wash accumulated [^{32}P]P_i and [γ-^{32}P]ATP from the filter at given times. The apparatus consists of a bell jar containing a circular array of receiving vials. A large inverted rubber stopper rests on the top opening of the bell jar, and embedded in this stopper is a filter holder (Swinnex) connected to an arm long enough to divert the filtrate to the receiving vials. A 1-mL

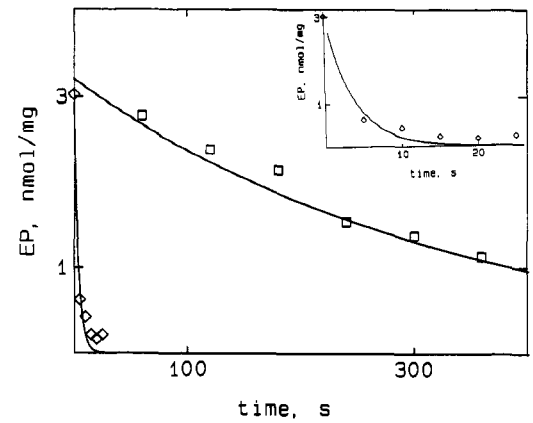

FIGURE 1: Effect of reactive red-120 on the time course of SR CaATPase EP hydrolysis. Phosphoenzyme decay was measured in the absence (◇) and presence (□) of 10 nmol mg^{-1} reactive red-120. The experimental procedure and reaction conditions are described under Materials and Methods. The lines were drawn by using the exponential fitting function and the fitted rate constants of 0.3 ± 0.1 and (3.7 ± 0.4) × 10^{-3} s^{-1} for the uninhibited and inhibited ATPase, respectively. Inset: expanded time course obtained in the absence of reactive red-120.

SR reaction solution containing the components in the previously mentioned concentrations was phosphorylated with 25 μM [γ-^{32}P]ATP and applied to the filter with house vacuum. The reaction was initiated by washing the filter with ice-cold nonradioactive solution containing the desired components. The arm was sequentially positioned over the other vials at given times and was washed with 1 mL of a given media; each collection took 2–3 s. These reactions were performed at 0 °C in the cold room.

A 0.5-mL aliquot of the filtrate was added to 0.5 mL of fined 10% (w/v) charcoal in 0.33 M HCl, vortexed, and centrifuged. The supernatant was analyzed for [^{32}P]P_i, and the charcoal was washed twice with 1 mL of cold water. To quantitate [γ-^{32}P]ATP production, the washed decanted charcoal in the microcentrifuge tube was capped and placed in a scintillation vial filled with water; Cerenkov radiation was determined by using the tritium channel (Chojnacki & Matysiak, 1971). The efficiency of Cerenkov counting was determined to be 8%. The capacity of the charcoal was checked to be sure that large amounts of added cold nucleotides did not interfere with [γ-^{32}P]ATP binding.

The data were fit with a BASIC computer program which uses a nonlinear regression algorithm (Marquardt, 1963; Bevington, 1969). For time course data, a fitting function for a first-order single exponential was used to obtain k_{obs}. The dependence on [L] of k_{obs} was fit to

$$k_{obs} = k_0(1 - \alpha) + k_{max}\alpha$$

where k_0 and k_{max} are the rate constants at zero and saturating ligand (L), respectively, $\alpha = [L]/(K_d + [L])$, and K_d is the apparent dissociation constant of L.

Results

In order to study the interactions of nucleotides with the phosphorylated intermediate of the SR CaATPase, it was necessary to slow down the reactions. This was done by adding the noncompetitive inhibitor reactive red-120 (Coll & Murphy, 1987). As can be seen in Figure 1, this inhibitor reduces the single-turnover rate of EP hydrolysis to only a few percent of the control reaction, thereby allowing manual collection of data. Varying the reactive red-120 concentration from 8 to 15 nmol (mg of SR protein)$^{-1}$ yielded the same rate of EP loss which indicates that the bound inhibitor allows the enzyme

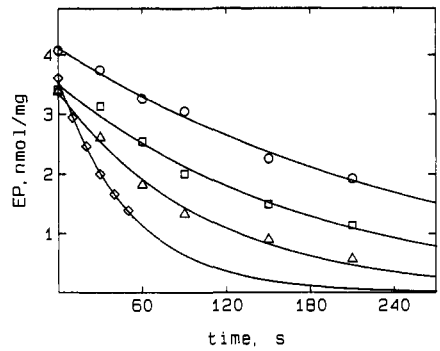

FIGURE 2: ATP-induced acceleration of the hydrolysis of preformed [^{32}P]EP. Representative time courses of EP decay at different ATP concentrations are shown. The procedure and experimental conditions are described under Materials and Methods; [NaCl] was kept constant as described under Results. The [ATP] and associated rate constants are as follows: zero (○), 0.004 ± 0.0004 s^{-1}; 0.1 mM (□), 0.006 ± 0.0008 s^{-1}; 1 mM (△), 0.009 ± 0.001 s^{-1}; 5 mM (◇), 0.02 ± 0.002 s^{-1}.

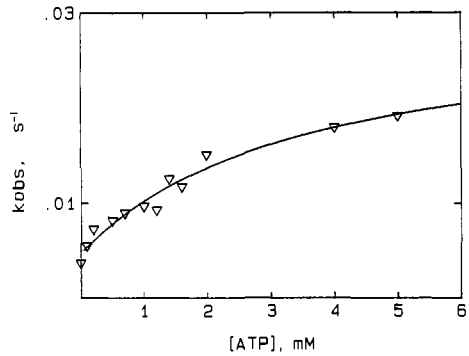

FIGURE 3: ATP concentration dependence of the rate constants for EP hydrolysis. The rate constants (k_{obs}) of EP decay were determined at several concentrations of ATP as described in Figure 2. The line was generated from the fitting function (see Materials and Methods) and the fitted parameters k_0 (rate constant in absence of ligand) = 0.005 ± 0.001 s^{-1}, k_{max} = 0.03 ± 0.008 s^{-1}, and K_{ATP} = 3.5 ± 1.2 mM.

to operate but at a greatly reduced rate.

Figures 2 and 3 characterize the interactions of added ATP with the reactive red-120 inhibited phosphoenzyme. The time courses in Figure 2 are well fit by a monoexponential function which includes the value of EP determined at zero time (prior to addition of EGTA and ATP). These reactions, while slowed by the inhibitor and low temperatures, are performed under normal maximizing solvent conditions: pH 7.0, high free [Mg^{2+}], and 80 mM KCl. Despite this, it was found that added salt caused increases in EP hydrolysis, perhaps by binding to a monovalent cation site on the enzyme or simply by increasing the ionic strength. The salt-caused increases in EP hydrolysis are very modest compared with the rate enhancement caused by nucleotide binding (17.5 mM NaCl causes approximately an 18% increase in rate, whereas 5 mM ATP causes approximately a 4-fold increase); however, ignoring the additional acceleration from the salt of neutralization adversely affected the goodness of fit. Therefore, the EP hydrolysis reaction mixtures were adjusted to a constant ionic strength with NaCl or Tris–HCl. For example, if the highest [ATP] was 5 mM, then all the lesser ligand reaction solutions would be adjusted to 17.5 mM final [NaCl].

Figure 3 shows the saturation plot for ATP-induced acceleration of EP hydrolysis. The determined binding constant is 3.5 mM, which is somewhat weaker than normally observed, and the rate enhancement was approximately 6-fold (most reported values range about 3–4-fold). The rate of EP hydrolysis measured from EP loss agreed well with that determined by P_i production using the aforementioned filtration device. When calcium-free phosphoenzyme was formed from P_i (de Meis & Inesi, 1982) and diluted into our normal reaction buffer, the resulting time course of EP loss was too fast for us to resolve. This means that the rate-limiting step which millimolar [ATP] activates involves a calcium-containing form of EP and this step is followed by the much faster hydrolysis of calcium-free phosphoenzyme. This is also the case for the uninhibited enzyme under these solvent conditions (de Meis, 1981).

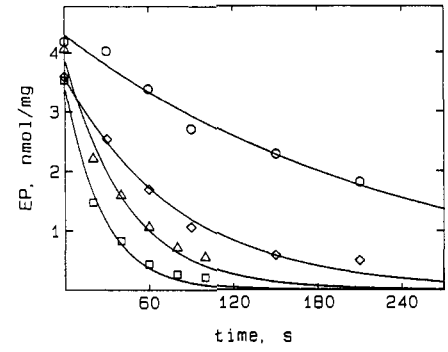

FIGURE 4: ADP-induced acceleration of EP dephosphorylation. Representative time courses of EP loss (ATP synthesis) at different concentrations of ADP are shown. The procedure and experimental conditions are stated under Materials and Methods. The concentrations of ADP and their associated rate constants are the following: zero (○), 0.004 ± 0.001 s^{-1}; 0.05 mM (◇), 0.01 ± 0.002 s^{-1}; 0.2 mM (△), 0.02 ± 0.004 s^{-1}; 3 mM (□), 0.04 ± 0.006 s^{-1}.

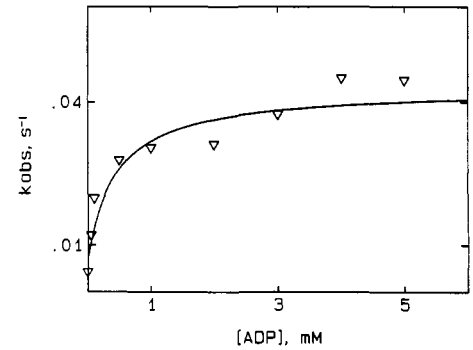

FIGURE 5: ADP concentration dependence for the ATP synthesis reaction. Values of k_{obs} were obtained as described in Figure 4. The line was generated from the fitting function (see Materials and Methods) and the fitted parameters k_0 = 0.008 ± 0.003 s^{-1}, k_{max} = 0.04 ± 0.01 s^{-1}, and K_{ADP} = 0.4 ± 0.2 mM.

The addition of ADP to the calcium-containing phosphoenzyme results in the synthesis of ATP. This reaction, followed by loss of EP, is shown in Figure 4. As can be seen, the loss of EP is well described by a single exponential; the zero time point falls on the regressed curves, giving no indication of an initial jump or lag. At each [ADP], the salt concentration was adjusted to be equivalent to that which is associated with 5 mM neutralized ADP. Figure 5 shows the saturation curve for the ADP-induced increase in EP loss; it yields a binding constant of about 0.5 mM and an approximately 5.5-fold increase in rate of EP loss.

In order to determine how ATP and ADP interact with the phosphoenzyme when added simultaneously, the ligands were added in concentrations above their K_d's and the rate of product release was followed. The interaction of 1 mM ADP with EP yielded a rate of 0.028 s^{-1} when EP loss was monitored (Figure 5) and a rate of 0.04 s^{-1} when ATP synthesis was monitored (Figure 6). The ATP synthesis rate is slightly higher because its reaction contains higher salt, equivalent to

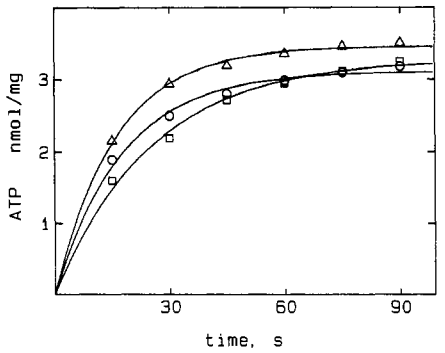

FIGURE 6: Effect of added ATP on the reaction of [^{32}P]EP with ADP. The time course of ATP synthesis was followed by using the procedures and conditions stated under Material and Methods; for all three conditions, the [NaCl] was equivalent to that of 10 mM neutral ATP. The production of [γ-^{32}P]ATP from 1 mM ADP was followed at the following [ATP] with their associated rate constants: zero (□), 0.04 ± 0.006 s^{-1}; 5 mM (○), 0.06 ± 0.008 s^{-1}; 10 mM (△), 0.06 ± 0.006 s^{-1}.

10 mM neutral ATP, and in between flushings the reaction in the filter is at 4 °C, whereas the EP loss reaction is continuously at 0 °C. Figure 6 shows that upon addition of 5 and 10 mM cold ATP with 1 mM ADP, the amount of [γ-^{32}P]-ATP synthesized does not decrease. The amounts of P_i released under these three conditions were similar and less than 0.5 nmol. The regressed lines did not assume zero ATP at zero time, so their convergence at that point indicates that there is no lag or early fast phase in ATP synthesis; added ATP enhanced the rate of ATP synthesis by 60%. This enhancement is not due to ADP contamination since HPLC showed the diphosphate was neither present in the added ATP nor produced by calcium-independent ATPase activity.

Discussion

Like other membrane ATPases, the calcium pump of SR exhibits biphasic kinetics when reaction velocity is measured as a function of [ATP]. The enzyme has a high-affinity (micromolar) regime in which the maximal level of covalent phosphoenzyme intermediate builds up (4–5 nmol mg^{-1}). Further increases in ATP concentration lead to turnover acceleration with a kinetic constant in the millimolar range. Studies have shown that virtually all the CaATPase can be isolated as the phosphoenzyme (Barrabin et al., 1984), and estimates of the amount of pump present in SR membranes come close to the measured value of steady-state EP (Coll & Murphy, 1984). These results rule out models involving alternating sites on oligomers and a single site which changes affinity during turnover, and indicate that the low-affinity acceleration of the rate-limiting step occurs by ATP binding to phosphoenzyme intermediate(s).

The physical basis of this low-affinity substrate effect has been widely sought; two possibilities are that it is due to ATP binding at the phosphorylated active site or at an allosteric site. FITC covalently labels lysine-515 of the ATPase and in so doing prevents the high-affinity binding and hydrolysis of ATP but allows enzyme phosphorylation by P_i (Andersen et al., 1982). EP formed from P_i has its hydrolysis rate stimulated by millimolar ATP, but FITC-labeled EP does not, which suggests that the phosphorylated active site is the regulatory site (Champeil et al., 1988). Other workers, using the fluorescent substrate analogue TNPAMP (Bishop et al., 1987), intramolecular cross-linking (Ross & McIntosh, 1987), or azido-TNPAMP (Seebregts & McIntosh, 1989), have also obtained results consistent with the phosphorylated active site being the regulatory site.

Scheme I

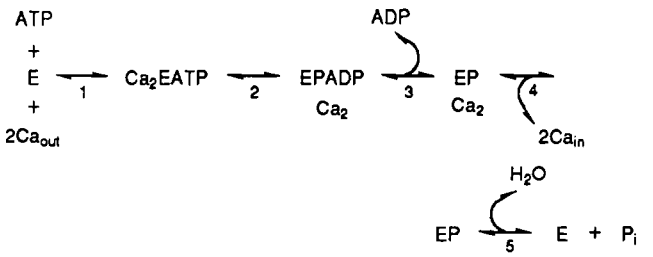

However, results of studies concerning the CaATPase interaction with its product, ADP, do not support the single-site model and are more easily understood in terms of the existence of an allosteric site for ATP acceleration. Pickart and Jencks (1984) studied the effect of [ATP] and [ADP] on equilibrium levels of EP; their results show very little effect of millimolar levels of ATP on EP level. According to their results, the equilibrium amount of EP seemed to be determined by [ADP], and added ATP did not prevent dephosphorylation of the enzyme. In addition, steady-state measurements of the pump hydrolyzing millimolar levels of ATP showed that added ADP produced noncompetitive inhibition which indicates that the two ligands act at spatially distinct sites (Coll & Murphy, 1985).

The present study is a continuation of attempts to gain information as to whether ATP activation of SR CaATPase turnover occurs via binding at the phosphorylated active site or at an allosteric site. Since ADP is the only substance unequivocally known to bind to the phosphorylated active site, it is of interest to observe how ATP, ADP, and EP behave in the forward and reverse reactions. Inhibition of the enzyme with reactive red-120 has allowed us to resolve the forward and reverse steps. The ATP synthesis reaction with the uninhibited enzyme is biphasic, with the first phase too fast to resolve (Pickart & Jencks, 1982); with the inhibited enzyme, the entire time course can be studied for mechanistic information (Figure 4). Although reactive red-120 may affect such properties as nucleotide affinity or magnitude of rate enhancement, the bound inhibitor would not change the site of nucleotide binding which is the topic of the present work. We will analyze the present results in terms of simple reaction schemes to see which are consistent with the data.

Scheme I presents the minimum necessary to describe the known steps in the SR CaATPase transport of calcium. Step 4, which involves the release of calcium into the lumen of SR, is rate-limiting under present conditions. It is followed by a much faster hydrolysis of the calcium-free phosphoenzyme (step 5). Activating ATP accelerates step 4, and this can be followed by measuring P_i or remaining phosphoenzyme. Reversal of the pump (ATP synthesis and release of calcium to the outside) is represented by steps 3 through 1: ADP binding to EP, ATP synthesis, and release of ATP. Under the present conditions, step 2 appears to be rate-limiting because the reversal monitored by loss of EP or ATP production gave close to the same rates. The forward and reverse reactions are characterized by Figures 3 and 5, respectively; it can be seen that both ADP and ATP bind to EP weakly. Assuming that binding of ligand is diffusion-controlled (1×10^9 M^{-1} s^{-1}), then ADP (K_d = 0.5 mM) would dissociate with a rate of 5×10^5 s^{-1}, and ATP (K_d = 3.5 mM) would dissociate with a rate of 3×10^6 s^{-1}. Even if the initial encounter complexes of the ligands with EP were to be followed by relatively slow conformational steps, the data indicate that the ligands will bind and dissociate thousands of times prior to undergoing a catalytic event.

Scheme II

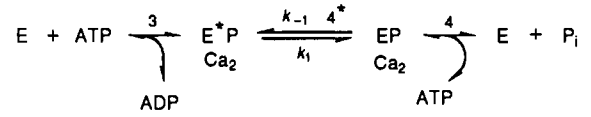

Scheme III

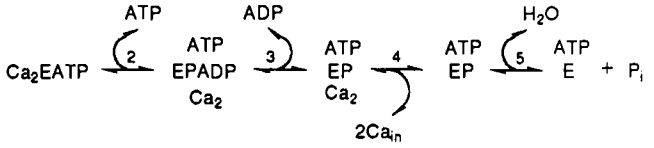

Perhaps the simplest mechanism for millimolar ATP activation of calcium transport is that after ADP leaves the phosphorylated active site it is replaced by ATP. The data in Figure 6 clearly show that this is not the case. Figure 6 shows that in the presence of 1 mM ADP (twice its K_d), EP decomposes with an almost stoichiometric production of ATP. When 5 or 10 mM ATP (2–3 times its K_d) is included, the amount of ATP synthesized is not decreased. Since ATP and ADP bind and dissociate rapidly to and from EP, they should compete for the same site and affect product distribution if this simple model were correct.[2]

A more elaborate mechanism for ATP activation of hydrolysis involves two forms of calcium-containing phosphoenzyme; one of them, E*P, only binds ADP and the other, EP, only binds ATP. The interconversion of these two phosphoenzyme forms is represented by step 4* in Scheme II. If the equilibration is fast relative to the catalytic events, then this scheme predicts competition between ATP and ADP, a phenomenon which is not observed. If the rate of interconversion between the two phosphoenzyme forms were close to or less than the catalytic rates, then the time courses for the forward and reverse reactions would yield distinctive patterns. For example, if we set k_{-1} equal to k_0 (hydrolysis rate in the absence of ligand = 0.004 s^{-1}) and look at the time course of phosphoenzyme loss in the presence of 1 mM ADP (k = 0.03 s^{-1}), then we should see an initial rapid drop in phosphoenzyme as ADP reacts with the E*P form and this would be followed by a slower loss as EP converts to E*P. The time courses shown in Figures 2 and 4 are monoexponential and show no obvious deviations one would expect from a [ligand]-independent phase. Another drawback to this single nucleotide binding site model is that it predicts that at any given time there will be a fraction of phosphoenzyme capable of binding ADP and a fraction capable of binding ATP. The data in Figure 6 show that upon simultaneous addition of ADP and ATP to the phosphoenzyme, virtually all of it reacts with ADP.

Under the present conditions, added ATP can accelerate EP hydrolysis by approximately 6-fold. This necessitates that the net rate for steps leading up to the rate-limiting step be at least 6-fold higher and thus the majority of EP is in a form which can bind ATP. Therefore, virtually all the EP can bind both ADP and ATP, and yet they do not compete when added simultaneously. We suggest that the simplest way to explain the observed behavior of EP with ADP and ATP is a two-nucleotide-site model as represented by Scheme III.

The [γ-^{32}P]ATP synthesis reaction (step 2) exhibits a modest 60% increase in rate upon addition of large amounts of cold ATP (Figure 6), indicating both ligands are bound simultaneously. The binding of ADP to the phosphorylated active site (step 3) is not inhibited by ATP as shown by the absence of a decrease in the rate of [γ-^{32}P]ATP production. The rate-limiting release of calcium from the phosphoenzyme (step 4) has been shown to be accelerated by millimolar [ATP] (Figures 2 and 3), and yet the presence of subsaturating [ADP] virtually prevents the phosphoenzyme from internalizing calcium as shown from the almost negligible production of P_i. We conclude that the acceleration of turnover observed in the presence of millimolar [ATP] is produced by ATP binding to a distinct allosteric site and not the phosphorylated active site. Given the similarity between the sodium–potassium and calcium ATPases (Pedersen & Carafoli, 1987; Green et al., 1988; Murphy, 1990), it is interesting that the former enzyme also shows evidence of a second nucleotide site (Askari & Huang, 1984).

Registry No. ATPase, 9000-83-3; ADP, 58-64-0; ATP, 56-65-5.

[2] To estimate how much of each product (P_i and ATP) is expected if ATP and ADP compete for the phosphorylated active site, we used the equation:

$$[\text{product}] = \frac{k_{max}[L]}{[L] + K_d(1 + [I]/K_i)}$$

Using the constants determined for hydrolysis (Figure 3) and ATP synthesis (Figure 5), we calculate that in the case of 1 mM ADP and 10 mM ATP the products would be 53% [γ-^{32}P]ATP and 47% [^{32}P]P_i.

References

Andersen, J. P., Moller, J. V., & Jorgensen, P. L. (1982) *J. Biol. Chem. 257*, 8300–8307.

Askari, A., & Huang, W. H. (1984) *J. Biol. Chem. 259*, 4169–4176.

Barrabin, H., Scofano, H. M., & Inesi, G. (1984) *Biochemistry 23*, 1542–1548.

Bishop, J. E., Al-Shawi, M. K., & Inesi, G. (1987) *J. Biol. Chem. 262*, 4658–4663.

Bowman, B. J. (1983) *J. Biol. Chem. 258*, 13002–13007.

Champeil, P., Riollet, S., Orlowski, S., Guillain, F., Seebregts, C. J., & McIntosh, D. B. (1988) *J. Biol. Chem. 263*, 12288–12294.

Chojnacki, T., & Matysiak, Z. (1971) *Anal. Biochem. 44*, 297–299.

Coll, R. J., & Murphy, A. J. (1984) *J. Biol. Chem. 259*, 14249–14254.

Coll, R. J., & Murphy, A. J. (1985) *FEBS Lett. 187*, 131–134.

Coll, R. J., & Murphy, A. J. (1987) *Biochim. Biophys. Acta 904*, 227–238.

de Meis, L. (1981) *The Sarcoplasmic Reticulum*, Wiley, New York.

de Meis, L., & Inesi, G. (1982) *J. Biol. Chem. 257*, 1289–1294.

Dupont, Y. (1984) *Anal. Biochem. 142*, 504–510.

Eletr, S., & Inesi, G. (1972) *Biochim. Biophys. Acta 282*, 147–179.

Green, N. M., Taylor, W. R., & MacLennan, D. H. (1988) in *The Ion Pumps: Structure, Function, and Regulation*, pp 15–24, Alan Liss, New York.

Gresser, M. J., Myers, J. A., & Boyer, P. D., (1982) *J. Biol. Chem. 257*, 12030–12038.

Hutton, R. L., & Boyer, P. D. (1979) *J. Biol. Chem. 254*, 9990–9993.

Inesi, G. (1985) *Annu. Rev. Physiol. 47*, 573–601.

Inesi, G., Goodman, J. J., & Watanabe, S. (1967) *J. Biol. Chem. 242*, 4637–4643.

Kanazawa, T., Saito, M., & Tonomura, Y. (1970) *J. Biochem. (Tokyo) 67*, 693–711.

Kirtley, M. D., Sumbilla, C., & Inesi, G. (1990) in *Intracellular Calcium Regulation*, pp 249–270, Alan Liss, New York.

Koland, J. K., & Hammes, G. G. (1986) *J. Biol. Chem. 261*, 12428–12434.
Lacapere, J.-J., & Guillain, F. (1990) *J. Biol. Chem. 265*, 8583–8589.
Marquardt, D. W. (1963) *J. Soc. Ind. Appl. Math. 11*, 431.
Moczydlowski, E. G., & Fortes, P. A. G. (1981) *J. Biol. Chem. 256*, 2357–2366.
Moulton, M. P., Sabbadini, R. A., Norton, K. C., & Dahms, A. S. (1986) *J. Biol. Chem. 261* 12244–12251.
Murphy, A. J. (1990) *FEBS Lett. 263*, 175–177.
Pedersen, P. L, & Carafoli, E. (1987) *Trends Biochem. Sci. 12*, 146–150.
Pickart, C. M., & Jencks, W. P. (1982) *J. Biol. Chem. 257*, 5319–5322.
Pickart, C. M., & Jencks, W. P. (1984) *J. Biol. Chem. 259*, 1629–1643.
Post, R. L., Hegvary, C., & Kume, S. (1972) *J. Biol. Chem. 247*, 6530–6540.
Richards, D. E., Rega, A. F., & Garrahan, P. J. (1978) *Biochim. Biophys. Acta 511*, 194–201.
Ross, D. C., & McIntosh, D. B. (1987) *J. Biol. Chem. 262*, 12977–12983.
Schuster, S. M., Ebel, R. E., & Lardy, M. A. (1975) *J. Biol. Chem. 250*, 7848–7853.
Seebregts, C. J., & McIntosh D. B. (1989) *J. Biol. Chem. 264*, 2043–2052.
Stieger, J., & Luterbacher, S. (1981) *Biochim. Biophys. Acta 641*, 270–275.
Wallmark, B., Stewart, H. B., Rabon, E., Saccomani, G., & Sachs, G. (1980) *J. Biol. Chem. 255*, 5313–5319.
Yamamoto, T., & Tonomura, Y. (1967) *J. Biochem. (Tokyo) 62*, 558–575.

Conformation of $NADP^+$ Bound to a Type II Dihydrofolate Reductase†

Rui M. M. Brito,‡ Frederick B. Rudolph,‡ and Paul R. Rosevear*
Department of Biochemistry, Rice University, Houston, Texas 77005, and Department of Biochemistry and Molecular Biology, University of Texas Medical School at Houston, Houston, Texas 77225
Received September 10, 1990; Revised Manuscript Received November 6, 1990

ABSTRACT: Type II dihydrofolate reductases (DHFRs) encoded by the R67 and R388 plasmids are sequence and structurally different from known chromosomal DHFRs. These plasmid-derived DHFRs are responsible for confering trimethoprim resistance to the host strain. A derivative of R388 DHFR, RBG200, has been cloned and its physical properties have been characterized. This enzyme has been shown to transfer the *pro-R* hydrogen of NADPH to its substrate, dihydrofolate, making it a member of the A-stereospecific class of dehydrogenases [Brito, R. M. M., Reddick, R., Bennett, G. N., Rudolph, F. B., & Rosevear, P. R. (1990) *Biochemistry 29*, 9825]. Two distinct binary RBG200·$NADP^+$ complexes were detected. Addition of $NADP^+$ to RBG200 DHFR results in formation of an initial binary complex, conformation I, which slowly interconverts to a second more stable binary complex, conformation II. The binding of $NADP^+$ to RBG200 DHFR in the second binary complex was found to be weak, $K_D = 1.9 \pm 0.4$ mM. Transferred NOEs were used to determine the conformation of $NADP^+$ bound to RBG200 DHFR. The initial slope of the NOE buildup curves, measured from the intensity of the cross-peaks as a function of the mixing time in NOESY spectra, allowed interproton distances on enzyme-bound $NADP^+$ to be estimated. The experimentally measured distances were used to define upper and lower bound distance constraints between proton pairs in distance geometry calculations. All $NADP^+$ structures consistent with the experimental distance bounds were found to have a syn conformation about the nicotinamide–ribose ($\chi = 94 \pm 26°$) and an anti conformation about the adenine–ribose ($\chi = -92 \pm 32°$) glycosidic bonds. The conformation of $NADP^+$ bound to RBG200 DHFR in the initial binary complex was qualitatively evaluated at 5 °C, to decrease the rate of interconversion to conformation II. The ratio of cross-peak intensities as well as the pattern of observed NOEs was only consistent with syn and anti conformations about the nicotinamide–ribose and adenine–ribose bonds, respectively, in the initial complex, conformation I. From the known stereochemistry of hydride transfer and the conformation of the enzyme-bound cofactor, a model is proposed for the orientation of cofactor and substrate at the active site of RBG200 DHFR. In this model, the NMNH moiety of NADPH is bound in a syn conformation with the pteridine portion of dihydrofolate located below the plane of the nicotinamide ring and rotated 180° with respect to dihydrofolate binding in chromosomal DHFRs.

Dihydrofolate reductase (DHFR; EC 1.5.1.3)[1] catalyzes a central reaction in one-carbon metabolism, the NADPH-dependent reduction of 7,8-dihydrofolate to 5,6,7,8-tetrahydrofolate. Chromosomal DHFRs are the target for a number of antifolate agents such as trimethoprim and methotrexate, which function by depleting the metabolic pool of one-carbon units necessary for normal cellular function. Type II DHFRs

† This work was supported by National Institutes of Health Grant GM 41232 to P.R.R., National Cancer Institute Grant 14030 to F.B.R., and grants from the Robert A. Welch Foundation, C-1041 and AU-1025 to F.B.R. and P.R.R., respectively.
* Author to whom correspondence should be addressed at the University of Texas Medical School at Houston.
‡ Rice University.

[1] Abbreviations: DHFR, dihydrofolate reductase; TMP, trimethoprim; MTX, methotrexate; DHF, 7,8-dihydrofolate; EDTA, ethylenediaminetetraacetic acid; DTT, 1,4-dithiothreitol; DSS, sodium 2,2-dimethyl-2-silapentane-5-sulfonate; DQCOSY, double quantum filtered two-dimensional correlated spectroscopy; NOESY, two-dimensional nuclear Overhauser enhancement spectroscopy; NOE, nuclear Overhauser effect; NMN, nicotinamide mononucleotide; AMN, adenine mononucleotide; TNOE, transferred nuclear Overhauser effect.

0006-2960/91/0430-1461$02.50/0